Astronomy Letters, Vol. 28, No. 1, 2002, pp. 49–62. Translated from Pis'ma v Astronomicheskiĭ Zhurnal, Vol. 28, No. 1, 2002, pp. 56–70.

HD 331319: A Post-AGB F Supergiant with He I Lines

V. G. Klochkova*, V. E. Panchuk, and N. S. Tavolzhanskaya

Special Astrophysical Observatory, Russian Academy of Sciences, Nizhnii Arkhyz, Stavropolskii Krai, 357147 Russia

Received April 26, 2001; in final form, August 8, 2001

Abstract—Based on CCD spectra taken with an echelle spectrometer attached to the 6-m telescope, we have determined for the first time the fundamental parameters and detailed chemical composition of HD 331319, an optical counterpart of the infrared source IRAS 19475 + 3119, by the model-atmosphere method. Helium lines were detected in the spectrum of this luminous ($Mv < -8^m$) object with the effective temperature $T_{\rm eff} = 7200$ K. This detection can be interpreted as a significant helium overabundance in the observed atmospheric layers and may be considered as a manifestation of helium synthesis during the preceding evolution. Nitrogen and oxygen were found to be overabundant, $[{\rm N/Fe}]_\odot = +1.30$dex and $[{\rm O/Fe}]_\odot = +0.64$dex, with the carbon overabundance being modest. The metallicity of the stellar atmosphere, $[{\rm Fe/H}]_\odot = -0.25$, differs only slightly from its solar value. The s-process metals are not overabundant but most likely underabundant relative to iron: $[X/{\rm Fe}]_\odot = -0.68$ for Y and Zr. Barium is also underabundant relative to iron: $[{\rm Ba/Fe}]_\odot = -0.47$. The heavier elements La, Ce, Nd, and Eu are slightly enhanced relative to iron: the mean $[X/{\rm Fe}]_\odot = +0.16$ for them. In general, the elemental abundances confirm that IRAS 19475 + 3119 is a post-AGB object. The metallicity in combination with the radial velocity $V_r = -3.4$ km s^{-1} and Galactic latitude $|b| = 2\overset{\circ}{.}7$ of the object suggest that it belongs to the Galactic disk population. The envelope expansion velocity, $V_{\rm exp\approx 21}$ km s^{-1}, was determined from the positions of the absorption bands that originate in the circumstellar envelope. A comparison of our results for the comparison star HD 161796 = IRAS 17436 + 5003, a typical post-AGB object, with previously published data revealed an evolutionary increase in the effective temperature of HD 161796 at a mean rate of $\geq 50°$ per year. © *2002 MAIK "Nauka/Interperiodica".*

Key words: *post-AGB supergiants, abundance determination*

1. INTRODUCTION

Nuclear reactions proceed in the interiors of stars as they evolve, which result, in particular, in the synthesis of helium nuclei. Therefore, it would be natural to use the spectra of evolved stars with various masses to determine the helium abundance. Determining the helium abundance for stars at various evolutionary stages has been the subject of many studies. However, as yet, there is no sufficient information on the helium enrichment of the atmospheric surface layers in post-AGB stars. Since these stars have already traversed a long evolutionary path (hydrogen and helium core and shell burning, mixing, and dredge-up) and passed through the stage of mass loss in the form of stellar wind on the asymptotic giant branch (AGB), there is every reason to expect a changed helium abundance in their atmospheres. Stars at the evolutionary stage of transition from AGB to a planetary nebula are commonly called post-AGB objects or protoplanetary nebulae (PPN).

We present the results of our spectroscopic analysis for the supergiant HD 331319, an optical counterpart of the IR source IRAS 19475 + 3119 (below referred to as IRAS 19475) whose spectrum was classified by Bidelman as F3 Ib [see the reference in Likkel *et al.* (1991)]. The energy distribution for HD 331319 has a double-peaked shape typical of post-AGB objects, which is attributable to an excess of the infrared flux emitted by the detached circumstellar envelope. The IRAS survey failed to resolve the nebula around HD 331319 (Young *et al.* 1993).

As a comparison object, we consider the well-known high-latitude superginat HD 161796, whose optical spectrum (F3 Ib) is similar to the spectrum of HD 331319. The supergiant HD 161796 is an optical counterpart of the IR source IRAS 17436 + 5003 (below referred to as IRAS 17436). Both these objects belong to reliable PPN candidates (Likkel *et al.* 1991). In the IR color–color diagram, IRAS 19475 and IRAS 17436 lie in region V (Loup *et al.* 1993).

Here, we determine the fundamental parameters, effective temperature $T_{\rm eff}$ and surface gravity $\log g$,

*E-mail: valenta@sao.ru

Table 1. A log of observations and the heliocentric radial velocities of IRAS 19475 measured from various features in its optical spectra

Spectrum	JD 2450000+	$V_\odot$, km s^{-1}						
		Metals, n	Blueward emission	$H\alpha$ abs	Redward emission	Na D1, D2	DIB (n)	
							IS	CS
s13203	0651.409	−2.0(187)	−41.4	+2.8	+57.2	−8.4	−11.2(4)	−24.3(1)
s26813	1651.575	−2.2(177)	−45.2	+1.8	+48.4	−8.6	−10.7(3)	−21.7(5)
s27323	1658.517	−4.6(33)	−41.0	+1.6	+42.0	−8.6	−11.8(6)	−21.3(1)
s27608	1708.451	−4.7(158)	−40.4	+2.3	+55.1	−7.4	−11.9(5)	−26.8(6)
Average, km s^{-1}		−3.4	−42.0	+2.1	+50.7	−8.2	−11.4	−24.2
$V_{\rm lsr}$, km s^{-1}		14.4	−24.2	+19.9	+68.5	+9.6	+6.4	−6.4

Note. The numbers in parentheses are the numbers of measured lines. The last row gives the velocities averaged over four spectra and corrected for solar motion toward the apex.

and compute the chemical composition (section 2). We also analyze the elemental abundances and the pattern of the radial velocities measured from various spectral features for the PPN candidate whose optical spectrum has not been studied previously (section 3). Our main conclusions are briefly summarized in section 4.

2. OBSERVATIONS, REDUCTION, AND ANALYSIS OF SPECTRA

We obtained the spectroscopic data at the prime focus of the 6-m (BTA) telescope using the PFES echelle spectrometer. The spectrometer and its capabilities were briefly described by Panchuk *et al.* (1998). The mean epochs of observations are given in Table 1. An echelle spectrum of the comparison star HD 161796 was taken on August 3, 1993. The signal-to-noise ratio for all the spectra used here significantly exceeds 100, which makes it possible to reliably measure the equivalent widths of weak lines up to 5–7 mÅ. The PFES echelle spectrometer is equipped with the 1160 × 1040-pixel CCD array (16 × 16 μm pixel size) designed at the Special Astrophysical Observatory. The PFES spectrometer provides a spectral resolution of $\sim$ 15000 simultaneously in the wavelength range 4550–7930 Å; the range limits can be changed. The reduction of two-dimensional images (the standard procedures of dark-current subtraction, cosmic-ray-particle hit removal, stray-light subtraction, and echelle-order extraction) was performed using the ECHELLE context of the MIDAS system (1998 version). We carried out spectrophotometric and position measurements on one-dimensional spectra with the DECH20 package (Klochkova and Galazutdinov 1991; Galazutdinov 1992).

The radial velocities measured from individual spectrograms of HD 331319 are given in Table 1. First, we singled out unblended lines by comparing the observed and synthetic spectra. The position zero point for each spectrogram was determined by the standard method, by tying in to the positions of ionospheric emissions of the night sky and the absorption telluric spectrum, which are observed against the background of the object's spectrum. When the number of lines exceeded 100, the error of the mean was typically $\delta = 0.3$ km s^{-1}, with the error of a single-line measurement being $\sigma \approx 2.5$ km s^{-1}. The average velocity derived from metal lines $Vr(\mathrm{met}) = -3.4$ km s^{-1}, which may be considered as the systemic velocity, is in good agreement for four epochs of observations. Consequently, the radial velocity of HD 331319 may be assumed to be nonvariable, within the limits of the measurement errors.

We found the main peculiarity, a complex absorption–emission $H\alpha$ profile, even in the first spectrum of HD 331319 (see Fig. 1). The second peculiarity of the HD 331319 spectrum is the presence of absorption features that coincide in position with He I lines (Fig. 2), which are normally absent in the spectra of such cool supergiants. The spectrum of HD 331319 is also remarkable in that the C I and O I lines belong to the strongest absorption features.

2.1. Determining the Model Parameters and Computing the Chemical Composition

To determine the fundamental parameters of model stellar atmospheres, effective temperature $T_{\rm eff}$ and surface gravity $\log g$, and to compute the chemical composition and synthetic spectra, we used the grid of model stellar atmospheres computed by Kurucz

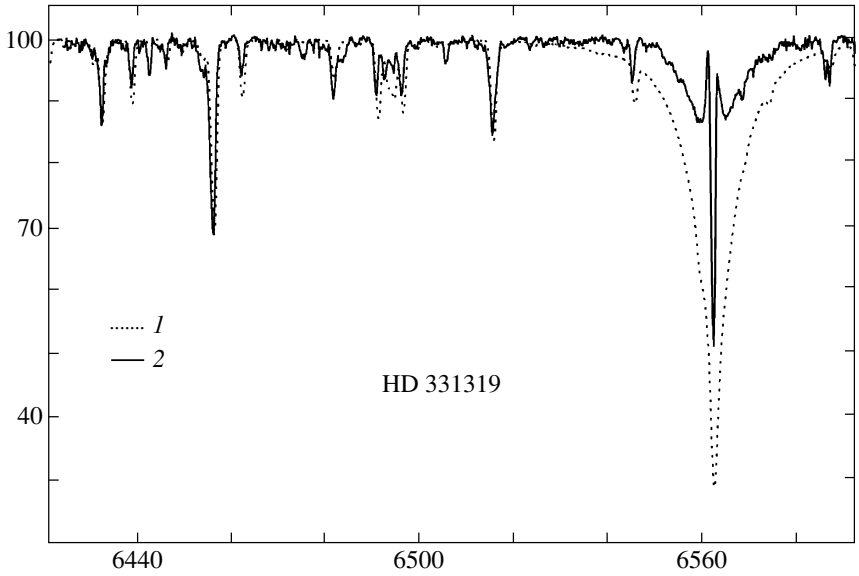

Fig. 1. Comparison of the theoretical (*1*) and observed, s26813, (*2*) spectra for HD 331319 near the $H\alpha$ line. The theoretical spectrum was computed with the parameters and chemical composition from Table 2. The helium abundance is solar.

(1993) in the hydrostatic approximation for various metallicities.

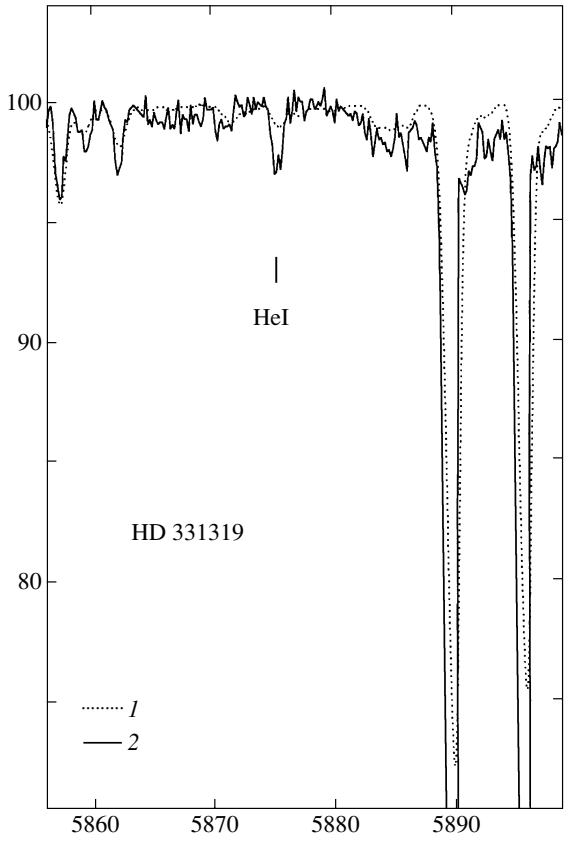

Fig. 2. Same as Fig. 1 for a wavelength range with the He 5876-Å line and the sodium doublet. The difference in the sodium-doublet intensities is attributable to the contribution of interstellar lines to the observed profile.

The effective temperature was determined by the standard method from the condition of the Fe I abundance being independent of the excitation potential for the corresponding lines. We chose the surface gravity from the condition of ionization balance for iron atoms and the microturbulence from the condition of the iron abundance being independent of the line intensity.

When determining the model-atmosphere parameters, we used low- and moderate-intensity lines with equivalent widths $W \leq 0.25$ Å. The approximation of a steady-state plane-parallel atmosphere may be inaccurate in describing the strongest spectral features. In addition, some of the strong absorption features could be distorted by the influence of the circumstellar envelope; at an insufficient spectral resolution, the intensities of envelope components are included in the intensities of atmospheric components.

The oscillator strengths gf of the spectral lines involved in determining the model parameters and elemental abundances were taken from Klochkova and Panchuk (1996) and Klochkova *et al.* (2000).

Thus, we determined the effective temperatures from the condition of the iron abundance being independent of the lower-level excitation potential for the lines used. An additional reliability criterion for the method is the lack of the same dependence for other chemical elements, which are also represented in the spectra by numerous lines (e.g., Si I, Ca I, Sc II, Ti II, Cr II, Ni I). In addition, for a reliable microturbulence determination, there is no dependence of individual abundances on the equivalent widths of the lines used in our calculations. The silicon abundances determined from lines of neutral atoms

Table 2. The chemical composition $\log \epsilon(X)$ of HD 331319 for two spectra and of the comparison star HD 161796 at $\log \epsilon(\mathrm{H}) = 12.0$

E	$\epsilon(E)^*$	X	HD 331319						HD 161796		
			s26813 7200K, 0.5, 5.0 km s^{-1},			s27608 7300K, 0.5, 6.0 km s^{-1}			s06401 7100K, 0.5, 6.0 km s^{-1}		
			$\epsilon(X)$	n	σ	$\epsilon(X)$	n	σ	$\epsilon(X)$	n	σ
He	10.99	He I	12.69	6	0.12	12.55	5	0.32	–	–	–
C	8.55	C I	8.39	22	0.24	8.50	20	0.24	8.52	5	0.14
N	7.97	N I	8.99	2	0.20	9.04	3	0.17	8.39	3	0.17
O	8.87	O I	9.41	3	0.12	9.17	3	0.12	9.15	2	–
Na	6.33	Na I	6.37	5	0.16	6.47	4	0.13	6.40	4	0.12
Mg	7.58	Mg I	7.31	3	0.24	7.16	3	0.25	7.26	1	–
Al	6.47	Al I	6.02	3	0.21	5.90	3	0.10	6.20	2	–
Si	7.55	Si I	7.80	22	0.23	7.73	20	0.18	–	–	–
		Si II	7.95	1	–	7.85	1	–	–	–	–
S	7.21	S I	7.38	6	0.20	7.36	5	0.08	7.46	6	0.20
Ca	6.36	Ca I	5.87	15	0.17	6.04	15	0.21	6.02	17	0.16
Sc	3.17	Sc II	2.43	12	0.21	2.44	8	0.18	2.43	6	0.26
Ti	5.02	Ti II	4.37	12	0.26	4.36	13	0.18	–	–	–
V	4.00	V II	3.36	3	0.18	3.42	3	0.14	–	–	–
Cr	5.67	Cr I	5.23	4	0.17	5.33	5	0.19	–	–	–
		Cr II	5.46	16	0.20	5.62	15	0.19	–	–	–
Mn	5.39	Mn I	5.59**	2	0.17	5.43**	4	0.33	–	–	–
Fe	7.50	Fe I	7.25	128	0.25	7.29	131	0.26	7.25	63	0.16
		Fe II	7.25	23	0.20	7.34	19	0.12	7.27	13	0.14
Ni	6.25	Ni I	6.10	13	0.23	6.35	26	0.29	6.28	12	0.37
Cu	4.21	Cu I	4.28	2	0.21	4.20	1	–	4.23	1	–
Zn	4.60	Zn I	4.41	3	0.25	4.41	3	0.35	4.63	1	–
Y	2.24	Y II	1.06	6	0.20	1.43	5	0.34	–	–	–
Zr	2.60	Zr II	1.79	3	0.21	1.80	1	–	–	–	–
Ba	2.13	Ba II	1.40	3	0.14	1.48	3	0.15	1.62	3	0.10
La	1.22	La II	1.22	5	0.25	1.31	4	0.03	–	–	–
Ce	1.55	Ce II	1.45	2	0.11	1.44	2	0.05	–	–	–
Nd	1.50	Nd II	0.91	3	0.08	1.72	4	0.27	1.58	1	–
Eu	0.51	Eu II	0.41	2	0.20	0.70	2	0.11	0.02**	1	–

Note. n is the number of lines used, and σ is the dispersion of the abundance derived for a given number of lines. Model parameters are given under the spectrum number.

* Data for the Sun from Grevesse *et al.* (1996).

** Uncertain values.

and ions are in agreement, within the accuracy of the method, suggesting that the atmospheric surface gravity was correctly estimated from the condition of ionization balance for iron atoms. The internal agreement between the parameters suggests that the homogeneous model atmospheres used are suitable for computing weak lines in the LTE approximation. The derived model-atmosphere parameters T_{eff}, $\log g$,

ξ_t, and elemental abundances $\epsilon(X)$ for each individual spectrum of the stars under study are given in Table 2. The elemental abundances relative to iron $[X/\mathrm{Fe}]_\odot$ are given in Table 3.

The low surface gravity, $\log g = 0.5$, agrees with the status of an F3 Ib supergiant obtained for HD 331319 from the spectral classification. We estimated the absolute magnitude M_V of the star from the equivalent width of the IR O I$\lambda \approx 7773$-Åtriplet. The equivalent width of this triplet, W(O I), can serve as a good criterion for the absolute luminosity of supergiants over a wide temperature range. In the spectrum of HD 161796, $W(\mathrm{O\,I}) = 2.2$ Å, which yields $M_V = -8^m$ when using the calibration of Slowik and Peterson (1995). In the spectrum of the star HD 331319 under study, the mean for three spectra is $W(\mathrm{O\,I}) = 2.6$ Å, which belongs to the extremely high observed values of W(O I). An even higher absolute magnitude $M_V < -8^m$ corresponds to this value. Unfortunately, since the set of UBV data required to estimate the color excesses is incomplete, we cannot determine the distance to the star. Clearly, the interstellar reddening in HD 331319 can be significant, because its Galactic latitude is low.

The typical accuracy of determining the model parameters (on average) for a star with a temperature of ≈ 7500 K is $\Delta T_{\mathrm{eff}} \approx 100$ K, $\Delta \lg g \approx 0.3$dex, and $\Delta\xi_t \approx 0.5$ km $^{-1}$. Most of the lines used to compute the chemical composition have equivalent widths less than 100 mÅ, which makes heavy demands on the accuracy of the observational data. The scatter of the elemental abundances derived from the set of lines is modest: the rms deviation σ typically does not exceed 0.25 dex (Table 2). All our calculations were performed with the WIDTH9 software package developed by Tsymbal (1996) in the LTE approximation. The corrections for hyperfine structure and isotopic shifts, which broaden Ni I, Mn I, and Ba II lines, were disregarded.

To check the reliability of our determination of the model-atmosphere parameters for HD 331319, we compared the observed spectrum of the object with its synthetic spectrum computed by using the STARSP code (Tsymbal 1996). The observed and theoretical spectra are compared in Fig. 1. For low- and medium-intensity absorption features, the agreement is satisfactory.

Table 3. Relative elemental abundances $[X/\mathrm{Fe}]$ in the atmospheres of the stars under study

Species	*HD* 331319	HD 161796	
	[Fe/H] = −0.25	−0.25	−0.32*
He I	+1.63	–	–
C I	+0.12	+0.21	+0.21
N I	+1.30	+0.90	+1.19
O I	+0.64	+0.53	+0.40
Na I	+0.31	+0.32	+0.51
Mg I	−0.12	−0.07	+0.75
Al I	−0.29	−0.02	–
Si I	+0.44	–	+0.45
Si II	+0.57	–	–
S I	+0.38	+0.50	+0.73
Ca I	−0.18	−0.09	−0.04
Sc II	−0.52	−0.49	−0.40
Ti II	−0.44	–	−0.47
V II	−0.39	–	–
Cr I	−0.16	–	–
Cr II	+0.08	–	+0.41
Mn I	−0.34**	–	–
Ni I	+0.19	+0.28	+0.53
Cu I	+0.25	+0.27	–
Zn I	+0.03	+0.28	+0.56
Y II	−0.78	–	−0.32
Zr II	−0.58	–	+0.12
Ba II	−0.47	−0.26	–
La II	+0.26	–	–
Ce II	+0.11	–	–
Nd II	+0.03	+0.33	+0.18
Eu II	+0.26	−0.24**	+0.15

* The data from Luck *et al.* (1990).
** Uncertain values.

3. DISCUSSION

3.1. Chemical Composition

For an enhanced helium abundance, the term 'elemental abundance' must be refined. In our algorithm for determining the chemical composition (Kurucz 1970; Tsymbal 1996), the abundance of a given element by the number of particles is normalized to the total number of atoms of all elements. Therefore, replacing a considerable fraction of hydrogen atoms with helium atoms does not lead to a renormalization of the abundances of the remaining chemical elements. The only case where a stipulation is required is the use of the designation [Fe/H] for HD 331319:

Table 4. Atmospheric light-element abundances $\epsilon(X)$ for HD 331319

λ	W, mÅ	$\log gf$	$\epsilon(X)$
He I 4471.473	64	−0.28	12.61
4713.140	28	−1.23	12.85
4921.930	20	−0.44	12.01
5875.620	38	0.41	12.55
7065.180	6	−0.46	12.73
C I 4775.900	37	−2.15	8.28
4817.370	15	−2.51	8.21
5039.050	38	−2.10	8.23
5041.660	111	−1.99	8.73
5052.150	103	−1.51	8.35
5380.320	56	−1.76	8.23
6014.840	11	−1.71	8.15
6108.530	6	−2.58	8.91
6587.620	59	−1.22	8.41
6605.800	9	−2.31	8.83
6711.300	8	−2.47	8.70
6828.120	33	−1.51	8.41
7085.470	4	−2.31	8.33
7100.300	45	−1.60	8.74
7108.940	45	−1.68	8.82
7111.480	64	−1.32	8.65
7113.180	87	−0.93	8.45
7115.190	92	−0.90	8.45
7116.990	92	−1.08	8.64
7119.670	58	−1.31	8.58
N I 7423.640	175	−0.61	9.09
7442.290	183	−0.31	8.85
7468.310	251	−0.13	9.17
O I 6155.980	131	−0.66	9.31
6156.770	144	−0.44	9.18
6158.180	151	−0.29	9.08

Note. The results of our calculations using spectrum s27608: $T_{\rm eff} = 7300$ K, $\log g = 0.5$, $\xi_{\rm t} = 6.0$ km s^{-1}.

it implies the Fe abundance measured for HD 331319 relative to the total number of H and He atoms, i.e., [Fe/H + He], but considered relative to Fe/H in the solar atmosphere. The meaning of all $[X/{\rm Fe}]$, which characterize the shape of the abundance curve, remains as before.

The elemental abundances $\log\epsilon(X) \pm \sigma$ averaged over the set of measured lines for the stars under study are given in Table 2. The second column in this table contains the corresponding data from Grevesse *et al.* (1996) for the solar atmosphere; we used these data to determine the relative abundances

$$[X/{\rm Fe}] = [\log\epsilon(X) - \log\epsilon(Fe)]_\star$$
$$= [\log\epsilon(X) - \log\epsilon({\rm Fe})]_\odot,$$

required to analyze the abundance curve. Blow, we consider the abundance pattern in the atmospheres of the two stars under study (see Tables 2 and 3).

Helium. The He I λ5876-Å line in the spectrum of HD 331319 was reliably measured for all epochs of observations: the mean equivalent width is $W = 38$ mÅ. We also detected other He I lines. Table 4 gives data on the measured He I lines in spectrum s27608 together with computed abundances. All the parameters of He I lines and lines of other elements in the vicinity of the He I lines that are required for our calculations were taken from the VALD database (Piskunov *et al.* 1995). The average helium abundance, $\epsilon({\rm He}) = 12.69$, for HD 331319 significantly exceeds its solar value, $\epsilon({\rm He})_\odot = 10.99$. This result needs to be comprehensively verified.

First, note that helium lines have been repeatedly observed in the spectra of post-AGB stars. Waelkens *et al.* (1992) detected the He I λ4471-Å line with the equivalent width $W = 23$ mÅ in the spectrum of HD 44179 (the central star of the Red Rectangle Nebula), which led the authors to conclude that the atmospheric helium is significantly enhanced. Van Winckel *et al.* (1996a) detected the He I $\lambda = 5876$-Å line with the equivalent width $W = 38$ mÅin the spectrum of HD 187885. The helium abundance in the atmosphere of HD 187885 with an effective temperature of ≈ 7700 K is significantly enhanced compared to its solar value. The above authors also ascribed a photospheric origin to the line. We measured the equivalent width of He I λ5876 Å in the spectrum of HD 187885, $W = 40$ mÅ, which is in excellent agreement with the data of Van Winckel *et al.* (1996a). Waelkens *et al.* (1991) reported on their measurement of the equivalent width $W = 15$ mÅ for He I λ4471 Å in the spectrum of HR 4049 with an effective temperature $T_{\rm eff} \approx 7500$ K. Van Winckel *et al.* (1996b) detected a very weak He I λ5876-Å line in the spectrum of the hotter ($T_{\rm eff} \approx 7800$ K) post-AGB star HD 133656, which led these authors to conclude that the helium abundance was solar. Having detected this line in the spectrum of HD 44179, we confirmed the result of Waelkens *et al.* (1992). Portions of the

spectra for HD 187885, HD 331319, and HD 44179 with the $\lambda = 5876$-Å line are shown in Fig. 3. Since we took the spectrum of HD 187885 ($\delta < -17°$) on June 5, 1996, with the PFES spectrometer at a large zenith distance, apart from stellar lines, numerous telluric lines are seen near the Na I doublet.

A conventional explanation of why there are helium lines in the spectra of cool stars is the assumption of an elevated excitation temperature, including the chromospheric hypothesis. The excitation temperature (or the effective temperature of a model atmosphere) can be estimated from line intensity ratios: if the lines are weak, then these ratios are only slightly sensitive to the elemental abundance. An extrapolation of the results by Auer and Mihalas (1973) to lower temperatures can be used to roughly estimate the equilibrium temperature. By analyzing the ratios of the singlet/triplet (4921/4471, 4921/5876, 4921/7065) equivalent widths and the triplet/triplet (5876/4471, 7065/4471) ratios, we conclude that the observed equivalent-width ratios correspond to temperatures that are no higher than 9000 K. The 4921/4713 and 4713/4471 ratios that contain the $\lambda = 4713$-Å line intensity give an uncertainty. An analysis of the catalog of He I lines in the spectra of 492 stars (Klochkova and Panchuk 1987, 1989) shows that the $\lambda = 4713$-Å line is unsatisfactorily described by the calculations of Auer and Mihalas (1973) in the LTE and non-LTE approximations (the observed values are almost twice the theoretical ones); therefore, we excluded the $\lambda = 4713$-Å line from our analysis. Thus, we find from the line intensity ratios that the He I level excitation temperature cannot exceed 9000 K in the LTE approximation, i.e., the hypothesis of a photospheric origin for the He I lines in HD 331319 is not rejected.

He I lines are enhanced in several massive A supergiants, which can be interpreted in terms of the model with a temperature inversion in the chromosphere [an estimate of the effect for the A0 Ia supergiant HD 7583 can be found in Wolf (1973)]. As applied to the low-mass F supergiant HD 331319, this hypothesis raises objections. First, even in the A2 Ia supergiant HD 160529, the variable Fe I lines that show splitting and the appearance of an emission component (Wolf 1974) are considered to be evidence of a chromosphere, which is not observed in the A0 Ia supergiant. When passing to an F supergiant, the chromospheric Fe II components must grow. However, both in disk F supergiants (Klochkova and Panchuk 1988a) and in HD 331319, we observe only normal photospheric Fe II lines. Second, the presence of a chromosphere in the A3 Ia supergiant HD 33579 is accompanied by the asymmetry of all absorption lines that was found by Wolf (1972)

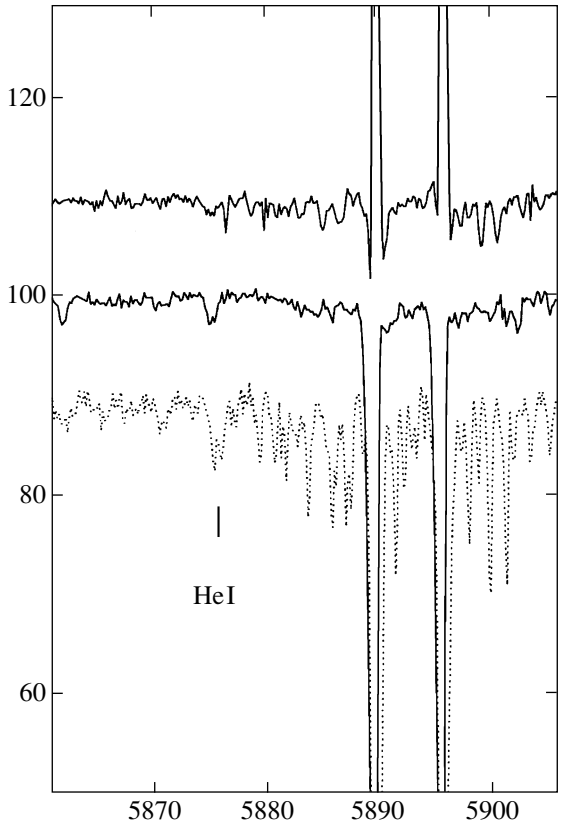

Fig. 3. A wavelength range with the He 5876-Å line and the sodium doublet in the spectra of three post-AGB stars, as constructed from our observations, from top to bottom: HD 187885, HD 331319, and HD 44179 (Red Rectangle). The spectrum of HD 187885 exhibits many telluric lines because of the large zenith distance of the star during our observations with the 6-m telescope.

with a spectral resolution lower than that in our study. For HD 331319, we found neither a line asymmetry nor a radial-velocity gradient. Third, line variability is considered to be evidence of the chromospheric contribution to the He I 5876-Å intensity, which is not observed in the spectra of HD 331319. Thus, there is no reason to suggest the presence in HD 331319 of a chromosphere similar to that discovered in A supergiants. Fourth, in the solar chromosphere, the triplet He I levels are an order of magnitude overpopulated compared to the singlet levels (Thomas and Athay 1965). By contrast, we observe an equilibrium population of the triplet and singlet levels in HD 331319 (see above) or at least equal singlet and triplet excitation temperatures. The observation of singlets with a highly reduced chromospheric contribution is the strongest evidence for the photospheric origin of the He I line.

Light elements. There is no Li I 6707-Å line in the spectrum of HD 331319, which can apparently be

explained by the total lithium destruction under convection conditions. In the spectrum of HD 161796, this line is very weak, but its equivalent width is measurable, $W = 3$ mÅ.

We reliably determined the carbon abundance [C/Fe] = +0.12 in the spectrum of HD 331319 from 22 C I lines. For He and CNO lines, Table 4 gives the measured and computed abundances for individual lines in one of the spectra (s27608). The derived carbon and helium abundances for HD 331319 are in good agreement with the [C/H]–[He/H] relation for B and A supergiants [see Fig. 12 in Takeda and Takada-Hidai (2000)]. The data of Waelkens *et al.* (1991) for the post-AGB star HD 52961 agree with this relation.

The N I 7423, 7442, and 7468-Å lines are also strong in the spectrum of HD 331319. Since their equivalent widths reach 200 mÅ, the nitrogen overabundance was determined reliably.

The oxygen abundance ([O/Fe] = +0.64) was computed by using the reliably measured O I lines at 6155 Å (see Table 4). The IR triplet lines are very strong in the spectrum of HD 331319, with their total equivalent width being $W = 2.6$ Å. Therefore, we did not use the triplet lines to determine the mean oxygen abundance, because in the LTE approximation, the oxygen abundance is derived from these lines for F supergiants with a very large systematic error (Gratton *et al.* 1999).

The revealed overabundances of the helium-burning products (carbon and oxygen) confirm the post-AGB stage for the two stars HD 161796 and HD 331319 under study. Note that our derived ratio O/C > 1 for HD 331319 is inconsistent with the absence of an OH band, as follows from radio observations of IRAS 19475 (Likkel 1989). According to the chronological sequence of Lewis (1989), the absence of an OH band in the spectrum of IRAS 19475 suggests that the object is close to the planetary nebula stage. At the same time, IRAS 17436 radiates in the masing OH 1667-MHz line, which is consistent with the atmospheric oxygen overabundance in the central star and which may point to an earlier time on the evolutionary path toward a planetary nebula. The presence of OH bands indicates an oxygen enrichment of the envelope. However, as Omont *et al.* (1993) emphasized, the absence of these bands only suggests a carbon enrichment of the envelope but cannot serve as its evidence.

Element Separation in the envelope. The object IRAS 19475 under study may be at the stage of intense mass transfer between the atmosphere and the circumstellar gas–dust envelope. The mere fact of a nearly solar iron abundance suggests that there are no severe distortions of the elemental abundances by condensation onto dust grains, because iron belongs to the elements with the most efficient settling on grains (Bond 1992). The CNO-group elements, sulfur, and zinc, which are essentially not subject to fractionation, exhibit a normal abundance (Bond 1992). Since the CNO abundances can change through nuclear reactions in the course of stellar evolution, the behavior of zinc and sulfur is critical in estimating the efficiency of selective separation.

A normal (relative to iron) zinc abundance, [Zn/Fe] = +0.03, was derived for HD 331319 from three lines, while in HD 161796, zinc is overabundant. The zinc abundance, which does not change during the stellar nucleosynthetis in the interiors of low- and intermediate-mass stars, varies by the same amount as the iron abundance over a wide metallicity range (Wheeler *et al.* 1989). Consequently, the conclusion regarding a zinc overabundance does not depend on the scale on which it was obtained (differential or absolute). This fact in combination with the normal ratio [Zn/Fe] = +0.03 leads us to conclude that there is no selective separation in the circumstellar envelope of IRAS 19475.

The sulfur abundance in the spectra of evolved stars seems to be a problem of its own. Bond and Luck (1987) found a large ([S/Fe] = +1.2) sulfur overabundance in the atmosphere of the metal-poor post-AGB star HD 46703 and explained it by the probable synthesis of sulfur through the attachment of α particles to C^{12} nuclei. However, Klochkova (1995) also discovered a sulfur overabundance in the atmosphere of the normal massive supergiant α Per. This star, on the one hand, has no circumstellar envelope and no condensation and, on the other hand, it would be unreasonable to expect any manifestations of the sulfur synthesis at such an early evolutionary stage. A sulfur overabundance seems to be a stable feature in the abundance pattern of evolved stars. In the atmospheres of unevolved stars, sulfur is also enhanced relative to iron (Timmes *et al.* 1995).

Light metals. Consider the behavior of the light-metal abundances for HD 331319. Sodium is slightly enhanced in the atmosphere of HD 331319, [Na/Fe] = +0.31, which could be a manifestation of the sodium synthesis during hydrogen burning. Mashonkina *et al.* (2000) showed that for a luminous star with $T_{\rm eff} \approx 7200$ K, allowance for sodium overionization results in sodium-abundance corrections of ≈ -0.15dex compared to the LTE approximation for subordinate lines.

>From the α-process elements, apart from sulfur, we determined the silicon, calcium, and titanium abundances. The abundance pattern in the atmospheres of HD 331319 and HD 161796 (Table 3) clearly shows a slightly reduced calcium abundance

and a more significant underabundance of scandium and titanium with differences in the zinc abundance.

The silicon overabundance, [Si/Fe] = = +0.5, was reliably determined for HD 331319 from two ionization states. Since only one, very strong Si II 6347-Å line was measured in the spectrum of HD 161796, the Si abundance was not determined for this star. However, Luch *et al.* (1990) give [SiI/Fe] = +0.45 for HD 161796, which is close to our value for HD 331319. Since the relative silicon abundance $[Si/Fe]_{\odot}$ in the atmospheres of unevolved stars with solar metallicity is nearly solar (Timmes *et al.* 1995), our data suggest that silicon is enhanced in HD 161796 and HD 331319. The anomalous abundances of silicon, calcium, scandium, and titanium can be a manifestation of the initial chemical peculiarities in HD 331319.

Iron-peak elements. For the iron-group metals, the two stars have a similar abundance pattern (Table 3). The mean abundance of the iron-group metals (vanadium, chromium, nickel) differs little from the iron abundance: [Met/Fe] = −0.07 for HD 331319. At the same time, individual iron-group elements exhibit significant overabundances and underabundances relative to iron. The chromium abundance agrees with its solar value. However, nickel, whose abundance was determined from a large set of Ni I lines, is slightly overabundant relative to iron, which corresponds to available data for unevolved stars with a nearly solar metallicity (Timmes *et al.* 1995). Copper is slightly enhanced in both stars, [Cu/Fe] ≈ −0.25; since this ratio was determined from one or two lines, its significance is low.

Heavy elements. It is generally believed (Blöcker 2001) that heavy metals could be overabundant in the atmospheres of post-AGB stars through neutronization, mixing, and dredge-up of the material that passed through these processes in the stellar interiors to the surface. However, contrary to the expected overabundance, the atmospheric barium abundance in HD 331319 reliably determined from three lines was found to be reduced. The relative abundances of the lighter s-process metals Y and Zr was determined with a lower accuracy because of the limited set of lines, but, in general, these metals can be said to be underabundant relative to iron, [s/Fe] = −0.68. For HD 161796, the light s-process metals Y and Zr (Luck *et al.* 1990) and Ba (our data) are also underabundant.

An underabundance of the s-process elements in the atmospheres of supergiants, including those at the post-AGB stage, is observed much more commonly than their overabundance (Klochkova and Panchuk 1988a, 1988b; Bond and Luck 1989; Van Winckel 1997; Klochkova 1998; Klochkova *et al.* 2001). We believe the observed lack of heavy-metal dredge-up manifestations to be real rather than the result of systematic errors in our analysis of the supergiant spectra by the model-atmosphere method. The presence or absence of an s-process underabundance is most likely to be somehow related to such fundamental stellar parameters as the initial stellar mass and mass-loss rate, which determine the course of evolution for a specific star. In the opinion of Garcia-Lario *et al.* (1999), the most massive and, hence, rapidly evolving post-AGB stars do not necessary have any s-process overabundance.

As for the group of heavier metals with $Z > 70$ (La, Ce, Nd, and Eu), which are predominantly synthesized in the r-process, our accuracy of determining their abundances is low because of the small number of weak lines. In general, however, these elements can be said to be slightly overabundant relative to iron, ≈ [heavy/Fe] = +0.16, in both stars.

Evolutionary manifestations of the chemical composition. Thus, neither lithium nor s-process elements were found to be overabundant in HD 331319. The only manifestation of the third dredge-up are the CNO-group overabundances. In general, the abundance pattern in the atmosphere of HD 331319 virtually coincides with that for the post-AGB standard HD 161796; except for an underabundance of the s-process metals, it is in good agreement with the views of a relatively massive star at the time of its post-AGB evolution. A substantial difference between HD 331319 and its counterpart is the presence of a significant helium overabundance in the atmosphere of this star. The high-latitude IR source IRAS 18095 + 2704, which Hrivnak *et al.* (1988) called the most likely PPN candidate, has similar characteristics [a similar abundance pattern (Klochkova 1995) and a featureless IR spectrum (Hrivnak *et al.* 1994)].

The spectral type of HD 331319 matches the spectral type F2–3 I determined by Parthasarathy *et al.* (1988) for HD 187885. These stars differ in metallicity only slightly: Van Winckel *et al.* (1996a) found iron to be slightly underabundant in HD 187885, [Fe/H] = −0.4. In addition, the atmospheres of both stars exhibit the same oxygen overabundance: [O/Fe] = +0.64, as inferred from our data for HD 331319, and [O/Fe] = +0.60 for HD 187885 from Van Winckel *et al.* (1996). This similarity is illustrated by Fig. 4, where portions of the spectra for HD 331319 and HD 187885 are compared.

While HD 331319 and HD 187885 are similar in metallicity and in helium and oxygen overabundances, there are also fundamental differences in the chemical compositions of these objects. HD 187885 has an atmosphere enriched with carbon (C/O > 1)

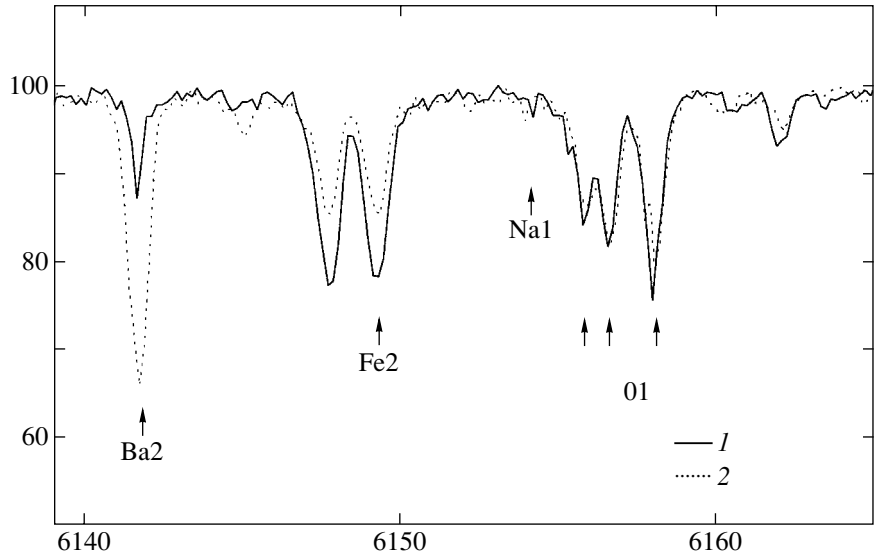

Fig. 4. A wavelength range with the O I ~ 6155-Å line in the spectra of two post-AGB звезд: HD 331319 (*1*) and HD 187885 (*2*).

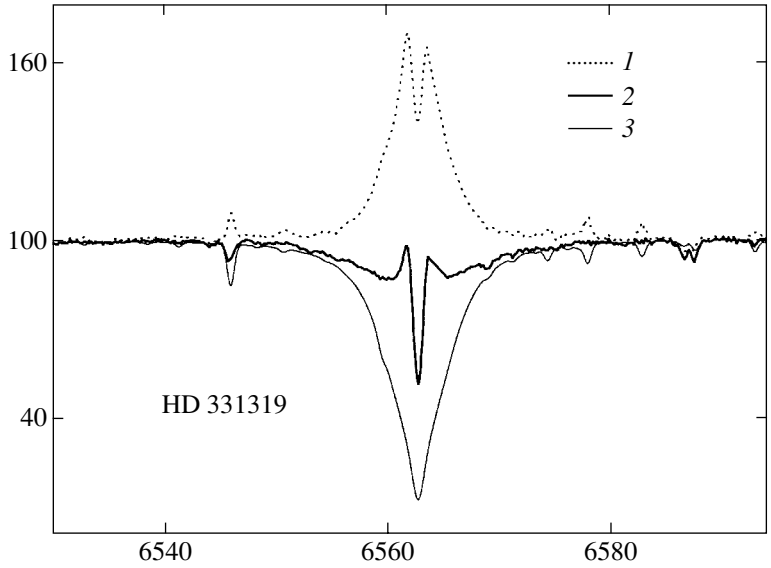

Fig. 5. Separating the emission (*1*) $H\alpha$ profile from the observed (*2*) spectrum of HD 331319. The synthetic spectrum is represented by a thin line.

and s-process metals. HD 187885 may be considered to be a standard post-AGB star whose atmosphere exhibits all the evolutionary changes in chemical composition that are expected at this stage. The IR spectra for the two compared stars also differ. The spectrum of the IR source IRAS 19500–1709, which is identified with HD 187885, shows a band near 21 μm that is absent in the spectrum of IRAS 19475. As was shown by Decin *et al.* (1998), Klochkova (1998), and Klochkova *et al.* (1999), there is a clear, but as yet incomprehensible relationship between the presence of the 21 μm band in the IR spectrum attributable to the circumstellar envelope and the existence of an atmospheric s-process overabundance in the central star.

3.2. Radial Velocities

To determine which type of Galactic population the object belongs to and to refine its evolutionary status requires additional information on its systemic velocity and on the velocity pattern in its atmosphere and envelope.

IRAS 19475 is a source of CO emission that originates in the expanding circumstellar envelope. Based on CO-band ($J = 1$–0) observations, Likkel *et al.* (1987) determined the systemic velocity of this source, $V_{\rm lsr} = 12$ km s^{-1}; Likkel *et al.* (1991) obtained $V_{\rm lsr} = 17.7$ km s^{-1} from CO-band ($J = 2$–1) observations. These values are close to the mean $V_{\rm lsr}({\rm met}) = 14.9$ km s^{-1} that we measured from metal lines. The derived equality between the radial velocities calculated for epochs separated by more than 10 years confirms our conclusion that the radial velocity of IRAS 19475 is nonvariable.

The $H\alpha$ line has a complex emission–absorption profile with absorption wings and two emission peaks with velocities that differ from the systemic velocity by -38 and $+54$ km s^{-1} (see Fig. 5 and Table 1). The velocity determined for the center of the Hα emission profile is equal to the velocity of the narrow absorption component.

As we see from Fig. 2, the profiles of the resonance Na D1 and 2 doublet lines are an unresolvable (at our spectral resolution) blend that includes stellar and interstellar components. We emphasize that the velocity measured from the He I 5876-Å line is equal to the mean velocity, which confirms its formation in the stellar photosphere.

Apart from photospheric absorption lines, we also detected several strong absorption features in the spectrum of HD 331319 whose positions allowed them to be identified with diffuse interstellar bands (DIBs). The equivalent widths of the most easily identifiable λ5780 and λ6613-Åbands are $W = 262$ and 80 mÅ, respectively. The band identification technique is the same as that used by Klochkova *et al.* (2000). The mean radial velocities measured from several features of this kind in each spectrum of HD 331319 are given in Table 1; there are two sets of bands in the spectrum of HD 331319, one is interstellar in origin (IS in Table 1) and the other (CS in Table 1) originates with a high probability in the circumstellar envelope. The velocity determined from the interstellar component and corrected for solar motion toward the apex is $V_{\rm lsr}({\rm IS}) = 6.4$ km s^{-1}. This value agrees with the results of Munüch (1957) for this direction in the Galaxy. Thus, the circumstellar absorption bands that were previously detected for several evolved stars (Cohen and Jones 1987; Le Bertre and Lequeux 1993; Klochkova *et al.* 2000; and references therein) were identified in the optical spectrum of yet another object (PPN candidate).

The difference between the radial velocities measured in the spectrum of HD 331319 from lines that originate in the photosphere and in the circumstellar envelope gives an envelope expansion velocity relative to the central star $V_{\rm exp} = 20.8$ km s^{-1}, which is a typical value for post-AGB stars. Our data on the expansion velocity obtained from optical lines and radio observations (Likkel *et al.* 1987, 1991) suggest that there is a velocity gradient in the circumstellar neighborhood of HD 331319, which is characteristic of low-mass post-AGB supergiants.

3.3. Hα Profile

Even far from the core, where the distortion by emission features does not show up clearly, the $H\alpha$ profile completely disagrees with the theoretical profile that was computed with the model parameters $T_{\rm eff}$ and $\log g$ determined from the star's "metallic" spectrum (Fig. 1). To explain such weak $H\alpha$ wings by the absorption alone requires lowering the effective temperature to the extent that the stellar metallicity will be one or two orders of magnitude larger than its solar value. Therefore, we propose to consider the observed $H\alpha$ profile as a superposition of two lines of different origin: a photospheric absorption component and an intense emission component with velocities in a wide range that originates in the circumstellar structure. In this case, the emission component can be separated from the observed profile by subtracting the theoretical photospheric profile from the observed one. If the photospheric profile computed using a model with a solar H/He ratio (indicated by the dotted line in Fig. 1) is subtracted from the observed profile, then the wings of the emission profile derived in this way extend to radial velocities of ± 1300 km s^{-1}. If we subtract the photospheric profile computed for an enhanced helium abundance, as shown in Fig. 5, then velocities of ± 450 km s^{-1} correspond to the farthest parts of the emission wings.

The double-peaked shape of the $H\alpha$ emission component suggests that the star is surrounded by a rotating disk, as in Be stars. If the emission wings are assumed to be Doppler ones, then we reach an absurd conclusion that the envelope (disk) rotates faster than the star. The intensity of the $H\alpha$ emission statistically weakens when passing from Be- to Ae stars simultaneously with decreasing mean projected rotational velocity, and the presence of $H\alpha$ emission in F stars is an exotic case. The emission-line width in the spectra of Be stars correlates with the absorption-line width; $H\alpha$ whose excessive width is commonly explained by electron scattering (Marlborough 1969; Poeckert and Marlborough 1979) constitutes an exception. At a temperature of 10 000 K, the mean thermal electron velocity is ± 400 km s^{-1}. By combining this estimate with the disk projected rotational velocity, which we estimated from the radial velocities of emission peaks to be 40 km s^{-1}, we obtain the observed wing width ± 440 km s^{-1}.

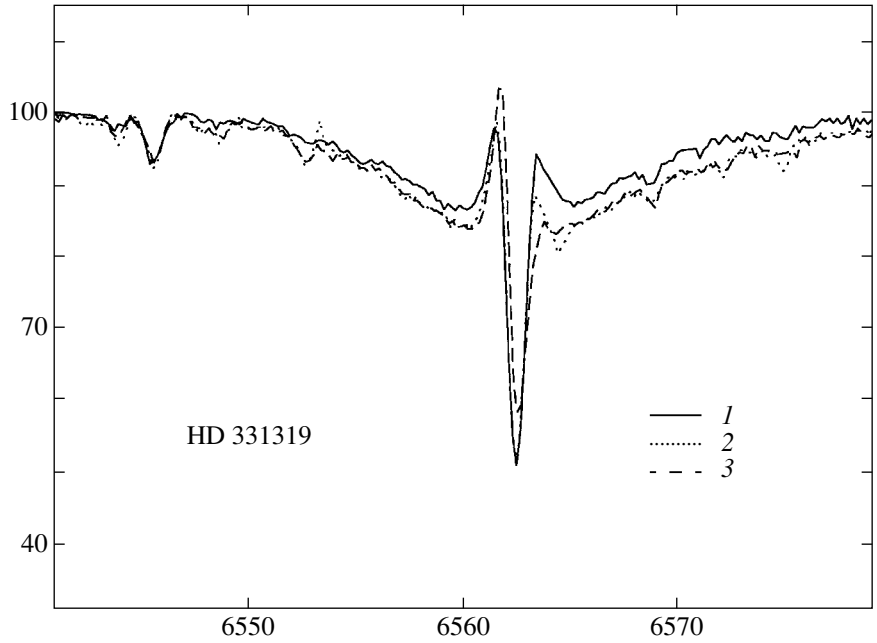

Fig. 6. Comparison of the $H\alpha$ profiles in the spectra of HD 331319 for three epochs of observations: *1* "— spectrum s261813, *2* "— spectrum s27323, and *3* "— spectrum s27608.

Observations show that the $H\alpha$ profile in the spectrum of HD 331319 changes with time: it follows from a comparison of the $H\alpha$ profiles for three dates in Fig. 6 that the intensity of the short-wavelength emission component increases simultaneously with decreasing intensity of the long-wavelength component.

3.4. Helium Atmosphere of an F Supergiant

The atmospheric structure of evolved stars with a changed H/He ratio has been previously considered by Sonneborn *et al.* (1979) in connection with the helium abundance in Cepheid envelopes and by Böhm-Vitense (1979) in connection with molecular-band intensity variations in globular-cluster giants. Since a changed helium abundance in the atmosphere of a post-AGB star is a reasonable assumption, we made some estimates.

For the temperature and luminosity of HD 331319, we used algorithms of solving the system of atomic ionization and molecular dissociation equations (Panchuk 1974) and algorithms of computing the continuum absorption coefficients (Panchuk 1975) for a gas mixture of 31 chemical elements. As a result, we obtained the following: when the helium abundance increases approximately by an order of magnitude, the combined effect on negative ions consists in reducing the absorption by two orders of magnitude at $\lambda < 1.67$ μm (at which the contribution of bound–free transitions to H^-) is largest) and by one and a half orders of magnitude at $\lambda > 1.67$ μm, with the contribution from free–free transitions to He^- being triple the H^- contribution. The contribution of absorption by neutral hydrogen is minor. The Thompson scattering decreases in importance by an order of magnitude because of the reduction in electron density. The Rayleigh scattering by helium atoms, with a small addition of scattering by carbon atoms, will dominate, but the total scattering coefficient will decrease approximately by a factor of 4 and will be insignificant compared to absorption even in the ultraviolet.

Our synthetic-spectrum calculations show that a general increase in the photospheric transparency causes the effective formation depths of weak lines and the wings of strong lines to increase. When gradually increasing the helium abundance, the wings of the Balmer hydrogen lines first strengthen (the Stark effect is stronger in denser atmospheric layers) and then weaken. Since denser layers are added to the line-forming region, the strengthening rates for metal and ionic lines are different. Our calculations indicate that the increase in mass of the absorbing layer above the photosphere, which results from the atmosphere becoming optically thin, is a few tenths of dex, and in no way can it offset the helium overabundance (1.6 dex) derived, to a first approximation, by using a model atmosphere with a solar H/He ratio. The computational effect of line strengthening clearly shows up for atomic lines of those elements that are predominantly in the ionized state (Li, Na). It may well

be that some of the individual chemical differences between post-AGB stars in the abundances of easily ionizable elements are attributable to variations in the atmospheric helium abundance of these stars.

3.5. The Temperature of HD 161796

We derived the same metallicity, [Fe/H] = −0.25, for both stars, HD 331319 and HD 161796. Based on the photographic spectrum of HD 161796 taken on August 1986, Klochkova and Panchuk (1988b) obtained $T_{\rm eff} = 6200$ K. Using a similar (spectroscopic) method of determining model parameters, Luck *et al.* (1990) derived the effective temperature $T_{\rm eff} = 6600$ K and metallicity [Fe/H] = −0.32 for HD 161796 from 1983–1986 spectrograms. The echelle spectrum taken on August 1993 yielded $T_{\rm eff} = 7100$ K, which significantly differs from the results for the mid-1980s. Thus, while the metallicities of HD 161796 are equal, within the accuracy of the method, the effective temperatures at different epochs differ significantly. This difference points to an evolutionary manifestation of the central star in IRAS 17436 when passing from AGB to a planetary-nebula nucleus. We believe that the effective temperature of the central star in IRAS 17436 increases at a mean rate of at least 50° per year.

4. CONCLUSIONS

We have presented the results of our spectroscopic analysis for the supergiant HD 331319, an optical counterpart of the IR source IRAS 19475 + 3119: we determined the model-atmosphere parameters, computed the detail chemical composition, and measured the radial velocities from various spectral features. The most important peculiarity of the optical spectrum for HD 331319 is a strong emission feature in the $H\alpha$ line and the presence of the reliably measured He I λ5876-Åabsorption line with the mean equivalent width $W = 38$ mÅin all spectra, which at a low temperature of the star suggests a large atmospheric helium overabundance, [He/Fe] = +1.63.

The detected small iron underabundance in the atmosphere of HD 331319, [Fe/H] = −0.25, reflects the initial chemical composition of the star, because the selective separation of elements in its circumstellar envelope was shown to be inefficient. The revealed overabundances of the helium-burning products (carbon and oxygen) suggest that the star HD 331319, whose optical spectrum has been studied for the first time, is at the post-AFB stage.

The metallicity in combination with the radial velocity and Galactic latitude of the object indicate that it belongs to the Galactic disk population. The envelope expansion velocity was found from the positions of the absorption bands originating in the circumstellar envelope to be $V \approx 21$ km $^{-1}$.

For the well-known protoplanetary nebula of HD 161796, which we consider as a typical and well-studied PPN candidate with parameters similar to those of the object under study, we found an evolutionary increase in the stellar effective temperature at a mean rate of 50° per year.

ACKNOWLEDGMENTS

The program of spectroscopic research on objects evolving away from AGB stars toward planetary nebulae with the 6-m telescope was supported by the Russian Foundation for Basic Research (project no. 99-02-18339) and the Federal Program “Astronomy” (project nos. 1.4.1.1 and 2.1.5.5). We used the SIMBAD, CDS, and VALD databases. The study whose results are presented here was supported, in particular, by the American CRDF Foundation (project no. RP1-2264).

REFERENCES

1. L. H. Auer and D. Mihalas, Astrophys. J., Suppl. Ser. **25**, 433 (1973).
2. E. Böhm-Vitense, Astrophys. J. **234**, 521 (1979).
3. T. Blöcker), Astrophys. Space Sci. **275**, 241 (2001).
4. H. E. Bond, Nature **356**, 474 (1992).
5. H. E. Bond and R. E. Luck, Astrophys. J. **312**, 203 (1987).
6. H. E. Bond and R. E. Luck, Astrophys. J. **342**, 476 (1989).
7. M. Cohen and B. F. Jones, Astrophys. J. **321**, L151 (1987).
8. L. Decin, H. van Winckel, C. Waelkens, *et al.*, Astron. Astrophys. **332**, 928 (1998).
9. G. A. Galazutdinov, Preprint No. 92 (Spets. Astrofiz. Obs., 1992).
10. P. García, F. D'Antona, J. Lub, B. Plez, and H. J. Habing, in *Proceedings of the 191st Symposium of International Astromonical Union "Asymptotic Giant Branch Stars", 1999,* Ed. by T. Le Bertre *et al.*, p. 91.
11. R. G. Gratton, E. Caretta, K. Eriksson, and B. Gustafsson, Astron. Astrophys. **350**, 955 (1999).
12. N. Grevesse, A. Noels, and A. J. Sauval, Astron. Soc. Pac. Conf. Ser. **99**, 117 (1996).
13. B. J. Hrivnak, S. Kwok, and K. M. Volk, Astrophys. J. **331**, 832 (1988).
14. B. J. Hrivnak, S. Kwok, and T. R. Geballe, Astrophys. J. **420**, 783 (1994).
15. V. G. Klochkova, Mon. Not. R. Astron. Soc. **272**, 710 (1995).
16. V. G. Klochkova, Bull. Spec. Astrophys. Obs. **44**, 5 (1998).
17. V. G. Klochkova and G. A. Galazutdinov, Preprint No. 71 (Spets. Astrofiz. Obs., 1991).

18. V. G. Klochkova and V. E. Panchuk, Soobshch. Spets. Astrofiz. Obs. **54**, 5 (1987).
19. V. G. Klochkova and V. E. Panchuk, Pis'ma Astron. Zh. **14**, 933 (1988a) [Sov. Astron. Lett. **14**, 395 (1988a)].
20. V. G. Klochkova and V. E. Panchuk, Pis'ma Astron. Zh. **14**, 77 (1988b) [Sov. Astron. Lett. **14**, 32 (1988b)].
21. V. G. Klochkova and V. E. Panchuk, Astrofiz. Issled. **27**, 25 (1989).
22. V. G. Klochkova and V. E. Panchuk, Bull. Spec. Astrophys. Obs. **41**, 5 (1996).
23. V. G. Klochkova, R. Szczerba, V. E. Panchuk, and K. Volk, Astron. Astrophys. **345**, 905 (1999).
24. V. G. Klochkova, R. Szczerba, and V. E. Panchuk, Pis'ma Astron. Zh. **26**, 510 (2000) [Astron. Lett. **26**, 439 (2000)].
25. V. G. Klochkova, V. E. Panchuk, and R. Szczerba, Astrophys. Space Sci. **275**, 265 (2001).
26. R. L. Kurucz, Smithsonian Astrophysical Observatory Special Report No. 309 (1970).
27. R. L. Kurucz, CDROMs (Smithsonian Astrophysical Observatory, Cambridge, 1993).
28. T. Le Bertre and J. Lequeux, Astron. Astrophys. **274**, 909 (1993).
29. L. Likkel, Astrophys. J. **344**, 350 (1989).
30. L. Likkel, A. Omont, M. Morris, and T. Forveille, Astron. Astrophys. **173**, L11 (1987).
31. L. Likkel, T. Forveille, A. Omont, and M. Morris, Astron. Astrophys. **246**, 153 (1991).
32. B. M. Lewis, Astrophys. J. **338**, 234 (1989).
33. C. Loup, T. Forvelle, A. Omont, and J. F. Paul, Astron. Astrophys., Suppl. Ser. **99**, 291 (1993).
34. R. E. Luck, H. E. Bond, and D. L. Lambert, Astrophys. J. **357**, 188 (1990).
35. J. M. Marlborough), Astrophys. J. **156**, 135 (1969).
36. L. I. Mashonkina, V. V. Shimanskiĭ, and N. A. Sakhibullin, Astron. Zh. **77**, 893 (2000) [Astron. Rep. **44**, 790 (2000)].
37. G. Münch, Astrophys. J. **125**, 42 (1957).
38. A. Omont, C. Loup, T. Forveille, *et al.*, Astron. Astrophys. **267**, 515 (1993).
39. V. E. Panchuk, Astrometr. Astrofiz. **22**, 37 (1974).
40. V. E. Panchuk, Astrometr. Astrofiz. **25**, 20 (1975).
41. V. E. Panchuk, I. D. Najdenov, V. G. Klochkova, *et al.*, Bull. Spec. Astrophys. Obs. **44**, 127 (1998).
42. M. Parthasarathy, S. R. Pottash, and W. Wamsteker, Astron. Astrophys. **203**, 117 (1988).
43. N. E. Piskunov, F. Kupka, T. A. Ryabchikova, *et al.*, Astron. Astrophys., Suppl. Ser. **112**, 525 (1995).
44. R. Poeckert and J. M. Marlborough, Astrophys. J. **233**, 259 (1979).
45. D. J. Slowik and D. M. Peterson, Astron. J. **109**, 2193 (1995).
46. G. Sonneborn, T. J. Kuzma, and G. W. Collins, Astrophys. J. **232**, 807 (1979).
47. Y. Takeda and M. Takada-Hidai, Publ. Astron. Soc. Jpn. **52**, 113 (2000).
48. R. N. Thomas and R. G. Athay, *Physics of the Solar Chromosphere* (Interscience, London, 1961; Mir, Moscow, 1965).
49. F. X. Timmes, S. E. Woosley, and T. Weaver, Astrophys. J., Suppl. Ser. **98**, 617 (1995).
50. V. Tsymbal, Astron. Soc. Pac. Conf. Ser. **108**, 198 (1996).
51. H. Van Winckel, Astron. Astrophys. **319**, 561 (1997).
52. H. Van Winckel, C. Waelkens, and L. B. F. M. Waters, Astron. Astrophys. **306**, L37 (1996a).
53. H. Van Winckel, R. D. Oudmaijer, and N. R. Trams, Astron. Astrophys. **312**, 553 (1996b).
54. C. Waelkens, H. van Winckel, E. Bogaert, and N. R. Trams, Astron. Astrophys. **251**, 495 (1991).
55. C. Waelkens, H. van Winckel, N. R. Trams, and L. B. F. M. Waters, Astron. Astrophys. **256**, L15 (1992).
56. J. C. Wheeler, C. Sneden, and J. W. Truran, Annu. Rev. Astron. Astrophys. **27**, 279 (1989).
57. B. Wolf, Astron. Astrophys. **20**, 275 (1972).
58. B. Wolf, Astron. Astrophys. **28**, 335 (1973).
59. B. Wolf, Astron. Astrophys. **36**, 87 (1974).
60. K. Young, T. G. Phillips, and G. R. Knapp, Astrophys. J., Suppl. Ser. **86**, 517 (1993).

Translated by V. Astakhov